Article

Not peer-reviewed version

Optical Imaging Provides a High Sensitivity at the Sensory-Motor Gyri: A Functional Approach

Estefania Hernandez-Martin *, Francisco Marcano, Oscar Perez-Diaz, Cristina De Dios, Jose Luis Gonzalez-Mora

Posted Date: 20 September 2023

doi: 10.20944/preprints202309.1247.v1

Keywords: diffuse optical imaging; functional-ROIs; structural-ROIs; sensory-motor activity; highly sensitive cerebral activations

Article

Optical Imaging Provides a High Sensitivity at the Sensory-Motor Gyri: A Functional Approach

Estefania Hernandez-Martin [1,2,*], Francisco Marcano [1,2], Oscar Perez-Diaz [1,2], Cristina de Dios [3] and Jose Luis Gonzalez-Mora [1,2]

[1] Department of Basic Medical Science (Physiology), Faculty of Health Sciences, Medicine Section, Universidad de La Laguna, 38071, Spain
[2] Instituto de Neurociencias, Universidad de la Laguna, Spain
[3] Arquimea Research Center, Las Mantecas, 38320, Santa Cruz de Tenerife, Spain
* Correspondence: ehernanm@ull.edu.es

Abstract: Diffuse optical tomography (DOT) technology enables a differentiation between oxyhemoglobin (HbO) and deoxyhemoglobin (HbR) in the sensory and motor cerebral gyri, resulting in greater sensitivity for cerebral activation compared to functional magnetic resonance imaging (fMRI). Here, we introduce a novel approach where functional regions of interest (ROIs) are created based on the specific signal behavior observed in DOT measurements, in contrast to the conventional use of structural-ROIs obtained from anatomical information. The generation of cerebral activation maps involves using the general linear model (GLM) to compare the outcomes obtained from both the functional and structural ROI approaches. DOT-derived maps are then compared with maps derived from fMRI datasets considered the gold standard for assessing functional brain activity. The results obtained demonstrate the effectiveness of employing functional ROIs to improve the spatial location of functional activations in the sensory and motor cerebral gyri by leveraging the neural synchronization data provided by DOT. Furthermore, this methodology simplifies data processing in animal models, where anatomical differences compared to the human head can pose challenges. By incorporating functional ROIs prior to GLM application, this study offers enhancements to DOT analysis techniques and broadens its applicability in both human and animal models.

Keywords: diffuse optical imaging; functional-ROIs; structural-ROIs; sensory-motor activity; highly sensitive cerebral activations

1. Introduction

Optical measurements play a crucial role in examining brain physiology, particularly in exploring the connection between neural activity and changes in hemodynamics. In neuroimaging studies, diffuse optical tomography (DOT) has been extensively utilized to detect functional alterations related to visual, motor, somatosensory, or cognitive stimuli [1]. Previous research has introduced a novel approach to processing DOT data, treating them as functional magnetic resonance imaging (fMRI) volumes. This approach was successfully validated in the prefrontal cortex using a cognitive paradigm [2] and in sensory and motor areas [3]. The DOT technique also enables precise measurement of hemodynamic changes during intricate brain processes, such as motor imagery, which reveals more subtle cerebral activations compared to motor execution [4].

The presence of signals from non-target anatomical regions, such as the scalp or the external layers of the skull, poses a significant challenge in DOT measurements. These signals introduce short-term variability that affects spatial and temporal changes throughout the brain and scalp [5]. To overcome this challenge, various methods have been employed that do not rely on assumptions about the hemodynamic model. Approaches like principal component analysis (PCA) or independent component analysis (ICA) have been utilized to generate cerebral activation maps [6] and reduce

 doi:10.20944/preprints202309.1247.v1

noise originating from these external layers. Similar to common practices in neuroimaging studies, a widely used method is region of interest (ROI) analysis, which relies on the structural anatomy of the brain. This approach involves selecting specific regions within the brain based on their anatomical landmarks or predefined brain atlases. By focusing on these regions of interest, researchers can analyze the DOT data specifically within these areas, allowing for more targeted and accurate examination of the functional activations. This structural-ROI based analysis in DOT is an approach commonly employed in neuroimaging studies, where researchers define specific regions of interest based on structural anatomy to investigate brain activity and connectivity patterns [7], particularly when a magnetic resonance (MR) device is available. However, a notable drawback of using DOT in human brain studies is the reliance on a structural MRI image for accurate localization of functional activations within the anatomy. This requirement for an MRI scan limits the usability of DOT techniques in situations where an MRI scan is not easily accessible.

Here, we investigate whether an ROI analysis could be constructed based on the intrinsic signal/brain characteristics across voxels, rather than relying on a structural-ROI. To test this hypothesis, we analyzed DOT data recorded from the well-studied sensory-motor area, where the spatial locations of activations are known. The data were collected from a group of healthy subjects while they performed finger movements with their right hands. The cerebral maps obtained from DOT were compared with the maps derived from fMRI data, providing a basis for comparison and validation.

2. Materials and Methods

2.1. Subjects and experimental design

A total of nine participants who were right-handed and had no history of neurological disease were included in the study. Prior to the experiment, the participants were given a thorough explanation of the procedures and purpose of the study, and they provided written consent to participate. The study received ethical approval from the local ethics committee at the University of La Laguna and was conducted in accordance with the guidelines stated in the Declaration of Helsinki.

A block design began with a 16 s resting condition, which consisted of the observation of a static word (Stop) in the center of the screen. The instructions appeared on the screen during all periods of each task block. The execution condition consisted of the performance of the opposition movement between the thumb finger versus the rest of the fingers for 16 s. A metronome set at 3 Hz was used for the execution condition. In order to stabilize physiological fluctuations and ensure steady-state magnetization of the tissue during fMRI, a 20-second dummy time was incorporated prior to each motor execution. The visual presentation of the experimental paradigm was facilitated through the use of Presentation software, developed by Neurobehavioral Systems, Inc., based in Albany, California. A total of twenty-four task blocks for each condition were performed with both DOT and fMRI devices. All instruments and facilities belonged to the Magnetic Resonance Service for Biomedical Research (Servicio de Resonancia Magnética para Investigaciones Biomédicas—SRMIB SEGAI)—at the University of La Laguna

2.2. Data acquisition and preprocessing in MRI

Functional magnetic resonance images were collected using a 3.0 T Signa Excite HD scanner manufactured by General Electric Healthcare. For precise anatomical localization, a T1-weighted volume was acquired with the following parameters: repetition time (TR) of 6 ms, echo time (TE) of 1 ms, flip angle of 12°, matrix size of 256 × 256 pixels, in-plane resolution of 0.98 × 0.98 mm, spacing between slices of 1 mm, slice thickness of 1 mm, and no interslice gap. The acquired anatomical slices encompassed the entire brain and were obtained parallel to the anterior-posterior commissure. During the motor paradigm, a series of 385 T2-weighted echo-planar imaging (EPI) volumes were obtained. The EPI sequence parameters included 36 axial slices covering the entire head, with a field of view of 25.6 mm, slice thickness of 4 mm, interslice gap of 1 mm, matrix size of 64 × 64, flip angle of 90°, repetition time (TR) of 2 seconds, and echo time (TE) of 22.1 ms.

Preprints (www.preprints.org) | NOT PEER-REVIEWED | Posted: 20 September 2023 doi:10.20944/preprints202309.1247.v1

The preprocessing of fMRI volumes was conducted using Statistical Parametric Mapping (SPM12) software developed by The Wellcome Trust Centre for Neuroimaging at University College London. The following steps were applied: realignment to correct for motion artifacts, slice timing correction, registration with the T1-weighted structural image, and transformation into the standard anatomical space of the Montreal Neurological Institute (MNI). To suppress noise and account for residual differences in functional and gyri anatomy, the EPI images were subjected to isotropic smoothing with an 8-mm full-width half-maximum kernel. Additionally, a high-pass filter with a cutoff period of 64 seconds was used to eliminate low-frequency noise associated with breathing and pulse signals [8].

2.3. Data acquisition and preprocessing for DOT measurements

To acquire the DOT (Diffuse Optical Tomography) data, a DYNOT 232 instrument manufactured by NIRx Medizintechnik GmbH in Berlin, Germany was utilized. The instrument employs continuous-wave measurements and operates with two laser sources at frequencies of 760 nm and 830 nm. The measurements were performed in a time-multiplexed scanning fashion, with a sampling rate of 1.8 Hz. For light transmission and detection, optical fibers (optodes) were used, allowing NIR light to travel to and from the DOT device. In this study, a total of thirty-two optical fibers were employed to measure hemodynamic changes in the contralateral cerebral hemisphere, specifically the left side. These optical fibers were configured as source-detector pairs, enabling the establishment of 1,024 optical channels to capture and analyze the diffuse optical signals. The optodes were arranged in a rectangular grid at a distance of 1 between each of them, covering the cover of the C3 position referring to the EEG 10-20 system [9] (Figure 1).

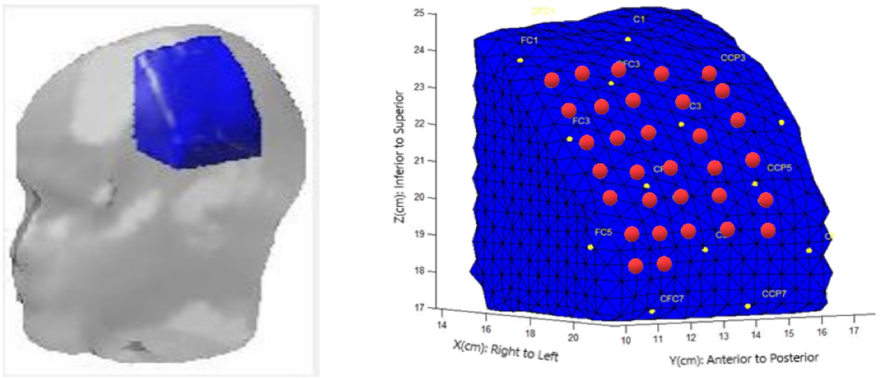

(**a**) (**b**)

Figure 1. Finite model element submesh selection. (**a**) Atlas with an FEM (blue) covering the sensory-motor cerebral area. (**b**) Localizations of optical fibers (circles) on the boundary. Red dots correspond to source-detector pairs.

DOT signals were preprocessed following the approach in prior studies that includes the following: 1) DOT signals were filtered using Bayesian filtering to remove physiological noise [10]; 2) optical fiber grid positions on individual heads were marked for a posterior translocation from individual space to precalculed forward model space from the BrainModeler tool from NIRx NAVI imaging; 3), the normalized difference method and minimum description length (MDL) were used as selection criteria for image reconstruction [2,4]. A total of 1,397 DOT volumes with a size of 64 × 64 × 64 voxels were reconstructed for each hemoglobin state (HbO & HbR).

2.4. Functional region of interest (Functional-ROIs)

Once DOT and fMRI data were preprocessed and normalized to standard MNI space, regional homogeneity [12] was calculated. This calculation is based on the assumption that brain regions involved in a particular function tend to exhibit similar temporal fluctuations in neural activity. This implies that neighboring voxels within a brain region should exhibit similar patterns of activity over

Preprints (www.preprints.org) | NOT PEER-REVIEWED | Posted: 20 September 2023 doi:10.20944/preprints202309.1247.v1

time. Therefore, regional homogeneity provides information about the coherence of neural activity within a specific brain region [11]. The time series for each voxel within the DOT-submesh is obtained by extracting the hemodynamic (BOLD, HbO and HbR) signals, which reflects changes in flow related to neural activity. Thus, for a voxel at time $V_{i=1,\dots,n}$ the rank R is defined as:

$$R = \frac{\sum_{i=1}^{n}(V)^2 - n(V)^2}{\frac{1}{12}C^2(n^3 - n)} \quad (1)$$

where *C* is the number of neighbors (7 voxels) of the voxel, n_i is the mean across its neighbors at the *i*th time point, and V is the overall mean rank across all neighboring voxels and time points. Besides, Kendall's coefficient (KCC) is used to measure the similarity of the time series among neighboring voxels within the ROI [12]. It determines the degree of concordance between the ranks of the time series data. Finally, the obtained KCC values are then transformed into Z-scores to allow for statistical comparisons based on one sample t-test (FWER-threshold p<0.001). As a result, the statistical maps of the group analysis, which spatially represent the synchronization of HbO, HbR, and BOLD signals within the DOT submesh, serve as functional-ROIs during the GLM calculation.

2.5. General linear model (GLM) for both fMRI and DOT data sets

The approach developed by the authors [2,4], to treat DOT volumes as if they were fMRI volumes using canonical SPM 12 software was used. In order to improve the signal-to-noise ratio, both the fMRI and DOT volumes underwent filtering by applying a high-pass filter based on discrete cosine transformation. The filter had a cutoff period of 64 seconds. The design matrix utilized in the analysis included two regressors: one for the rest condition and another for the task condition. These regressors were convolved with the canonical hemodynamic response function (HRF). It is worth noting that the convolutions were reversed to visualize the negative response corresponding to the HbR signal. Once the estimation was performed, cerebral activation maps were generated using a fixed effects model analysis. To specifically examine the motor execution condition compared to the rest condition, a contrast was computed. This resulted in the production of T-contrast maps for each dataset in both the DOT and fMRI modalities.

3. Results

Cerebral maps, generated through GLM analysis incorporating both structural and functional ROIs, were visualized using XjView 8.1 for measurements obtained from DOT and fMRI.

3.1. GLM analysis for the fMRI and DOT data sets using structural region of interest

Previous research has revealed that during finger-to-thumb opposition movements, the primary sensorimotor cortex (SMC) exhibits contralateral activation, which extends throughout the pre- and postcentral gyri. A GLM analysis using a structural-ROI (see Figure A1) was calculated to ensure the results for the following analysis steps using the same data set. As expected, Figure 2 shows the cerebral activations across the left pre- and postcentral gyri, covering the following Brodmann areas (BAs): BA2 and BA3, which correspond to the primary somatosensory cortex, and BA4 related to the motor cortex (M1).

Figure 2 shows t-maps for the BOLD (FWER-threshold p<0.05; [Peak MNI coordinates: -46; -18; 28]), HbO (FWER-threshold p<0.05; [Peak MNI coordinates SMC: -24; -32; 52, M1: -55; -18; 37]) and HbR (FWER-threshold p<0.05, [Peak MNI coordinates SMC: -44; -27; 54, M1: -23; 3; 49]) signals in coronal and axial views on the contralateral side.

Preprints (www.preprints.org) | NOT PEER-REVIEWED | Posted: 20 September 2023 doi:10.20944/preprints202309.1247.v1

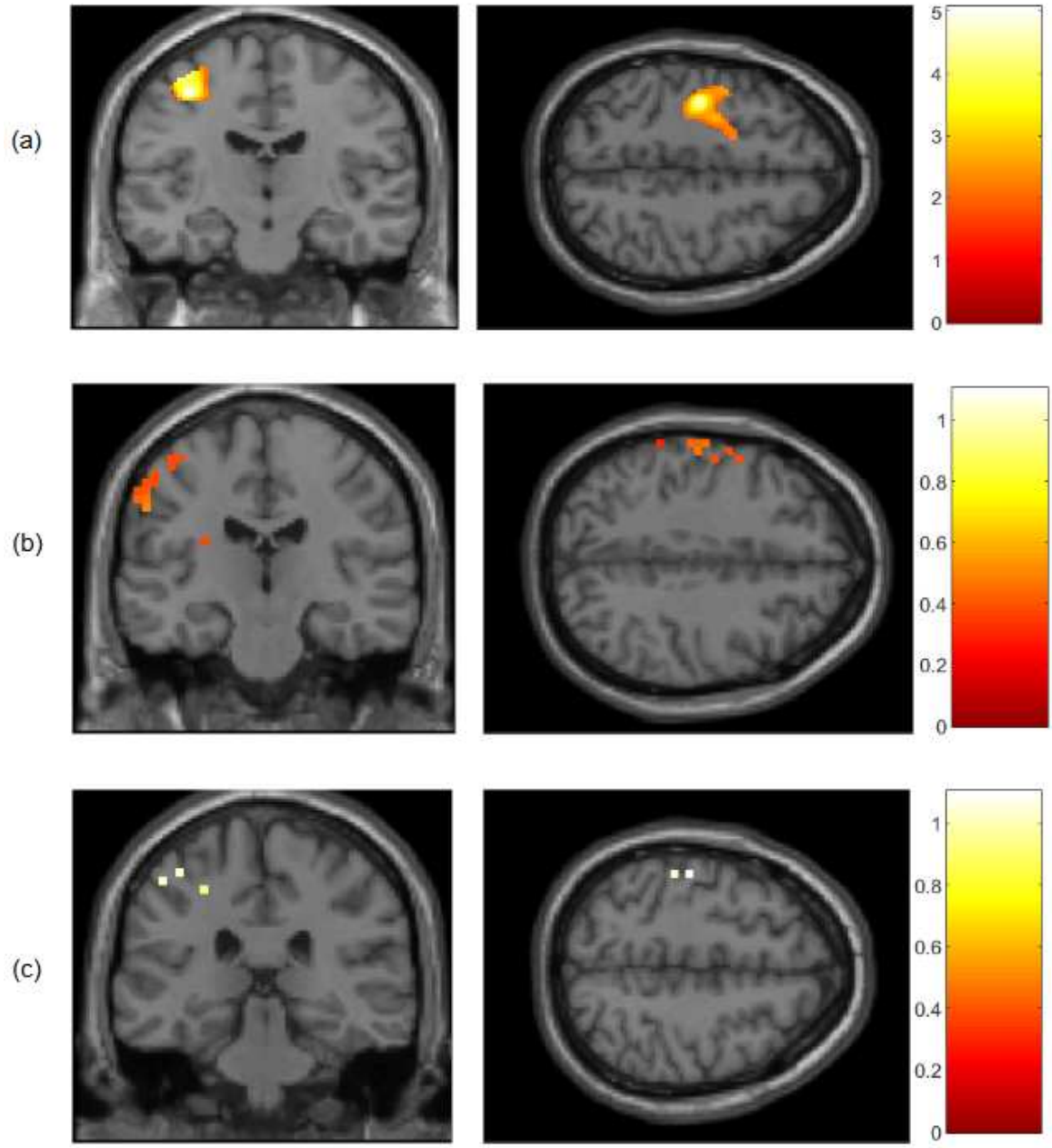

Figure 2. t-contrast maps of cerebral activation for the motor execution > rest contrast measured by the fMRI and DOT devices in a subject group (N = 9) for (**a**) BOLD, (**b**) HbO and (**c**) HbR signals in coronal and axial views. All results were mapped onto a standard space (MNI). FWER-threshold $p<0.05$ at the voxel level for all signals.

3.2. GLM analysis for the fMRI and DOT data sets using the functional region of interest

The resulting t-maps reveal robust cerebral activations in the contralateral pre- and postcentral gyri, specifically in Brodmann areas 1, 2, 3, 4, and 6, for both HbO and HbR (see Figure A2).

Compared to the GLM based on structural-ROI, GLM using functional-ROI seems to be less sensitive to constant event-related hemodynamic responses. However, its major advantage is the ability to detect unpredicted (event-nonrelated) hemodynamic responses that the GLM structural-ROI method itself failed to identify. Unpredicted hemodynamic responses combined with event-related hemodynamic responses help to understand the high complexity of human brain function, reaching the highest spatial resolution for loci at the gyri level. Figure 3 shows t-maps calculated on functional-ROIs corresponding to BOLD (FWER-threshold $p<0.05$, [Peak MNI coordinates: -36; -16; 52]), HbO (FWER-threshold $p<0.05$, [Peak MNI coordinates: -43; -34; 57]) and HbR (FWER-threshold

Preprints (www.preprints.org) | NOT PEER-REVIEWED | Posted: 20 September 2023 doi:10.20944/preprints202309.1247.v1

p<0.05, [Peak MNI coordinates: -39; -34; 61]) signals in coronal and axial views on the contralateral side.

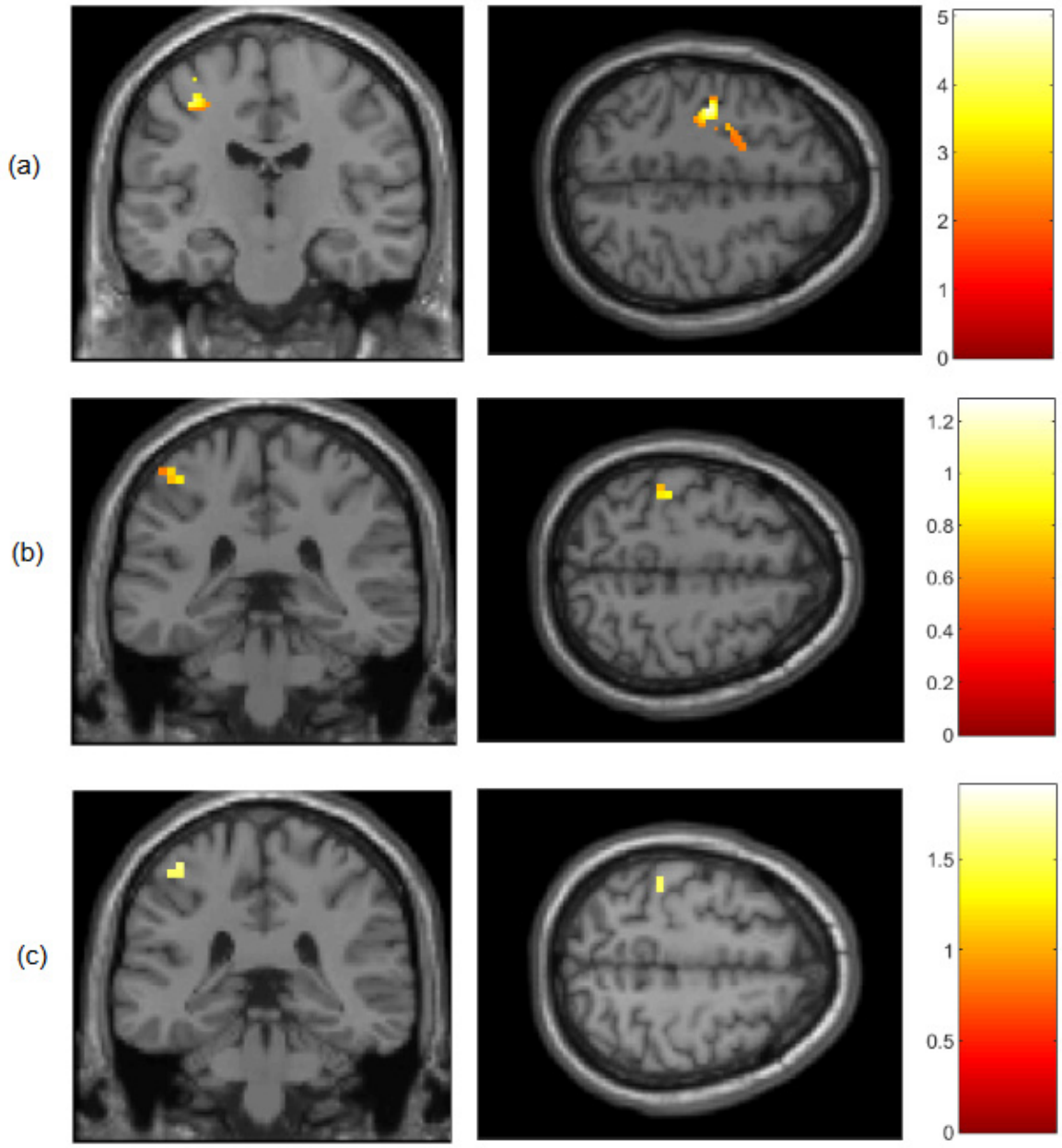

Figure 3. T-contrast maps of cerebral activation using ReHo maps as ROIs for the motor execution > rest contrast measured by the fMRI and DOT devices in a subject group (N = 9) for (**a**) BOLD, (**b**) HBO and (**c**) HbR signals in coronal and axial views. All results were mapped onto a standard space (MNI). FWER-threshold p<0.05 at the voxel level for all signals. The color bar depicts the signal changes.

3.3. Comparison structural and functional ROIs

3.3.1. Frequency domain analysis

Regional homogeneity analysis relies on assessing the temporal homogeneity of a voxel and its neighboring voxels, independent of the hemodynamic model employed by the GLM. Consequently, the signal dynamics of these voxels were analyzed using both structural and functional regions of interest (ROIs) for all signals. Figure 4 shows a frequency analysis revealing a main peak at 0.03 Hz (corresponding to the task which lasted 16 s) and well-represented by GLM analysis. However, the

Preprints (www.preprints.org) | NOT PEER-REVIEWED | Posted: 20 September 2023 doi:10.20944/preprints202309.1247.v1

magnitude of task frequency (0.03) is also increased in the GLM analysis when the functional-ROI is applied (max 0.35), (Figure 4b) in contrast to the structural-ROI GLM analysis (max 0.2) (Figure 4a).

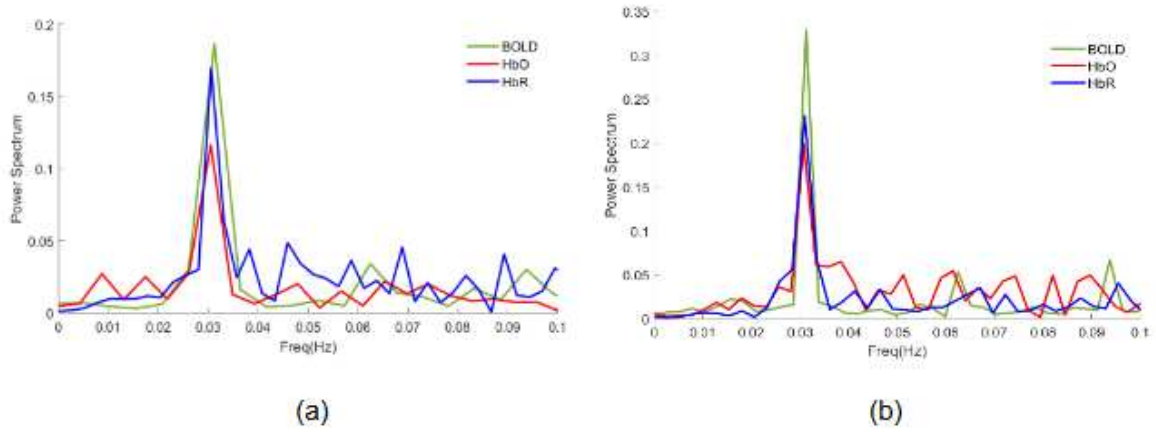

Figure 4. Power spectrum for the time series of BOLD (green lines); HbO (red lines); HbR (blue lines) signals in the cerebral activation maps generated by (**a**) GLM using structural-ROI, (**b**) GLM using functional. Vertical axis: Normalized Power Spectrum; Horizontal axis: Frequency (Hz).

3.3.2. Images analysis

Figure 5 shows that optical imaging, combined with the utilization of a functional-ROI is capable of detecting subtle variations in the lateral distribution of activation foci. Moreover, these brain regions are situated within deep sulcal structures, posing challenges for optical approaches to access them. The loci distributions for both the GLM using a structural-ROI and GLM using a functional-ROI results are along the sensorimotor and motor cortices.

Although the activation patterns show the strongest qualitative similarities in both methods, consistent differences worth mentioning were also observed. GLM using functional-ROI shows the major number of voxels distributed across the postcentral gyri (BA1, BA2 and BA3), which covers the primary somatosensory cortex for DOT and fMRI measurements. This fact matches prior studies in fMRI during finger tapping, which showed higher regional homogeneity in the sensory cortex than in the motor cortex itself [13]. The premovement sensory cortex shows a slight delay in encoding information about the impending activity of the forelimb muscles compared to the motor cortex. As a result, the sensory cortex receives information regarding motor output before the arrival of sensory feedback signals. This suggests that sensory processing engages in real-time processing of somatosensory signals through interactions with anticipatory information [14].

Preprints (www.preprints.org) | NOT PEER-REVIEWED | Posted: 20 September 2023 doi:10.20944/preprints202309.1247.v1

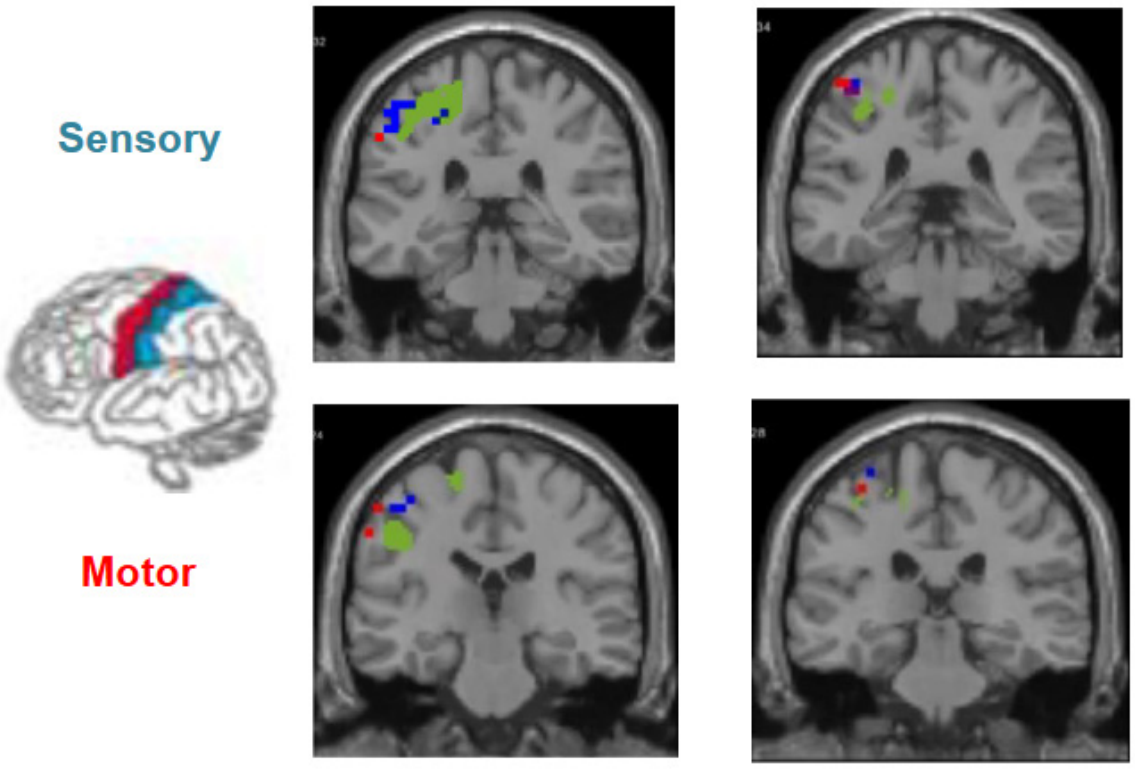

Figure 5. T-contrast maps measured by DOT and fMRI devices in a subject group (N = 9) on the left hemisphere localized on the postcentral gyri (upper figure) and the precentral gyri (bottom figure). All results were mapped onto a standard space (MNI) and statistically analyzed by GLM using a structural-ROI (left images) and GLM using a functional-ROI (right images). FWER-threshold $p<0.05$ at the voxel level for motor execution > rest contrast. BOLD (green), HbR (blue) and HbO (red) signals are displayed in coronal view.

4. Discussion

Finger tapping tasks are widely utilized in neuroimaging studies to investigate somatosensory and motor functions. This choice is primarily due to the higher amplitude of cerebral activations observed during finger tapping compared to other paradigms, such as cognitive tasks. Additionally, the spatial distribution of cerebral activations elicited by finger tapping is well-established and reproducible.

Firstly, regional homogeneity can be used to create a functional-ROI, in contrast to using structural anatomy to mask the background signals that are mixed with external layers (skull and scalp). The results presented here demonstrate that applying regional homogeneity to DOT volumes enables the attainment of precise cerebral activation information at the level of the gyri. This approach effectively eliminates extracerebral signals and does not rely on structural anatomy, which can be particularly challenging in situations where MRI devices are unavailable. This phenomenon can be attributed to the nature of regional homogeneity analysis, which captures not only task-related neuronal activity but also spontaneous neuronal activity that contributes to task-related activations. Additionally, regional homogeneity analysis may reveal shared neurovascular coupling mechanisms involved in both synchronized spontaneous and task-related activities. Here, we demonstrate the strong reliability of regional homogeneity analysis when applied to DOT volumes by comparing it with fMRI volumes.

As we expected, the outcomes obtained from the GLM analysis using a structural-ROI (Figure 1) align with previous research conducted on both fMRI and DOT datasets [3,4]. These studies have specifically focused on the sensory-motor cortices, namely the pre- and postcentral gyri. Furthermore, the regional homogeneity analysis (Figure A2) also aligns with previous fMRI studies [13,15] that have investigated sensorimotor areas during finger movements. It is noteworthy that no bandpass

 doi:10.20944/preprints202309.1247.v1

filtering was applied in this study, and the results revealed a higher correlation between HbR- BOLD signal compared to the correlation between HbO-BOLD signal [16,17]. These findings suggest that finger movements may impact signal synchronization across a wide range of frequency bands, including very low frequencies (<0.01 Hz), which significantly contribute to the observed results [13]. These collective findings provide strong evidence supporting the reliability and validity of applying regional homogeneity analysis to DOT volumes. Therefore, they further reinforce the viability and usefulness of employing this approach (functional-ROI) in the context of DOT.

Secondly, the results obtained from the GLM analysis using a functional-ROI reveal detailed cortical activation patterns in the pericentral motor and somatosensory cortices during task performance (Figure 5). Previous fMRI studies have demonstrated that these functional maps bear striking similarity to Penfield's electrophysiological maps, suggesting that noninvasive techniques can access the homuncular organization in healthy adults [17,18]. The findings presented in this study validate similar approaches utilizing high-density optical imaging [14]. By combining a functional ROI approach with a model-driven analysis (GLM), it becomes possible to accurately localize major cerebral activations in the pre- and postcentral gyri across a group of subjects while they perform contralateral movements, using both neuroimaging technologies. This methodology yields a spatial distribution of activations that aligns with the anatomical homuncular organization in the pre- and postcentral gyri. It is important to note that, in this study, individual finger movements cannot be distinguished. However, the results demonstrate the spatial localization of general finger movements, which is consistent with a recent study presenting an integrated-isolate model of action and motor control [19].

In conclusion, the fine-grained resolution of functional cortical activations presented here, along with several advantages such as non-invasiveness and safety, makes it suitable for specific clinical applications where other imaging methods may not be feasible. These applications include patients with medullary lesions, brain injuries, or muscle atrophy, allowing them to interact with their environment, especially during movements. Additionally, the potential applications of optical technology in monitoring hemodynamic changes for controlling robotic structures, particularly in the context of brain-computer interfaces (BCIs) and exoskeletons, are noteworthy. Moreover, this approach can provide valuable insights, particularly when animal models are employed to test and develop new technologies. Animal models may have limited access to neuroimaging tools for creating structural anatomical ROIs, making functional ROIs based on neural synchronization a more accessible and convenient option when working with DOT technology. Considering the less invasive nature of optical technology compared to electrophysiological microarray implants, future research should prioritize the design of brain implants based on optical technology for recording inputs from the sensorimotor cortex.

Author Contributions: E.H.M conceptualization, data analysis. data interpretation and original draft preparation, C.D project administration, E.H.M, F.M and O.P.D analyzed the data, C.D, F.M and J.L.G.M conducted the experiment. E.H.M., F.M and J.L.G.M review and editing. All authors contributed to the final manuscript.

Funding: Co-funded regional financing with European Regional Development Funds (ERDF). Consejería de Economía y Empleo, Agencia Canaria de Investigación, Innovación y Sociedad de la Información. Ref: ProID2021010096, 2021-2023. European funding, Convocatoria para la Recualificación del Sistema Universitario Español; NextGenerationEU. European Regional Development Fund (MAC/1.1b/098); Cooperation Program Interreg MAC II(Madeira-Azores-Canarias) 2014-2020.

Informed Consent Statement: Informed consent was obtained from all subjects involved in the study.

Data Availability Statement: Data underlying the results presented in this paper are not publicly available at this time but can be obtained from the authors upon reasonable request.

Acknowledgments: We express our sincere gratitude to the volunteers who generously participated in this study. We would also like to extend our thanks to Jose Maria Perez Gonzalez for his invaluable assistance with data acquisition. Additionally, we appreciate the English review and edits provided by Patrick Dennis.

Conflicts of Interest: The authors declare no conflict of interest.

Preprints (www.preprints.org) | NOT PEER-REVIEWED | Posted: 20 September 2023 doi:10.20944/preprints202309.1247.v1

Appendix A

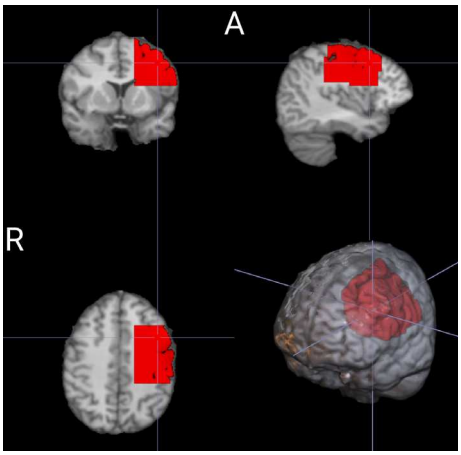

Figure A1. The structural-ROI (red) represents the selected submesh from the BrainModeler atlas in standard MNI space. This ROI encompasses the left pre- and post-sensorimotor and motor gyri, excluding external layers like the skull and scalp.

Appendix B

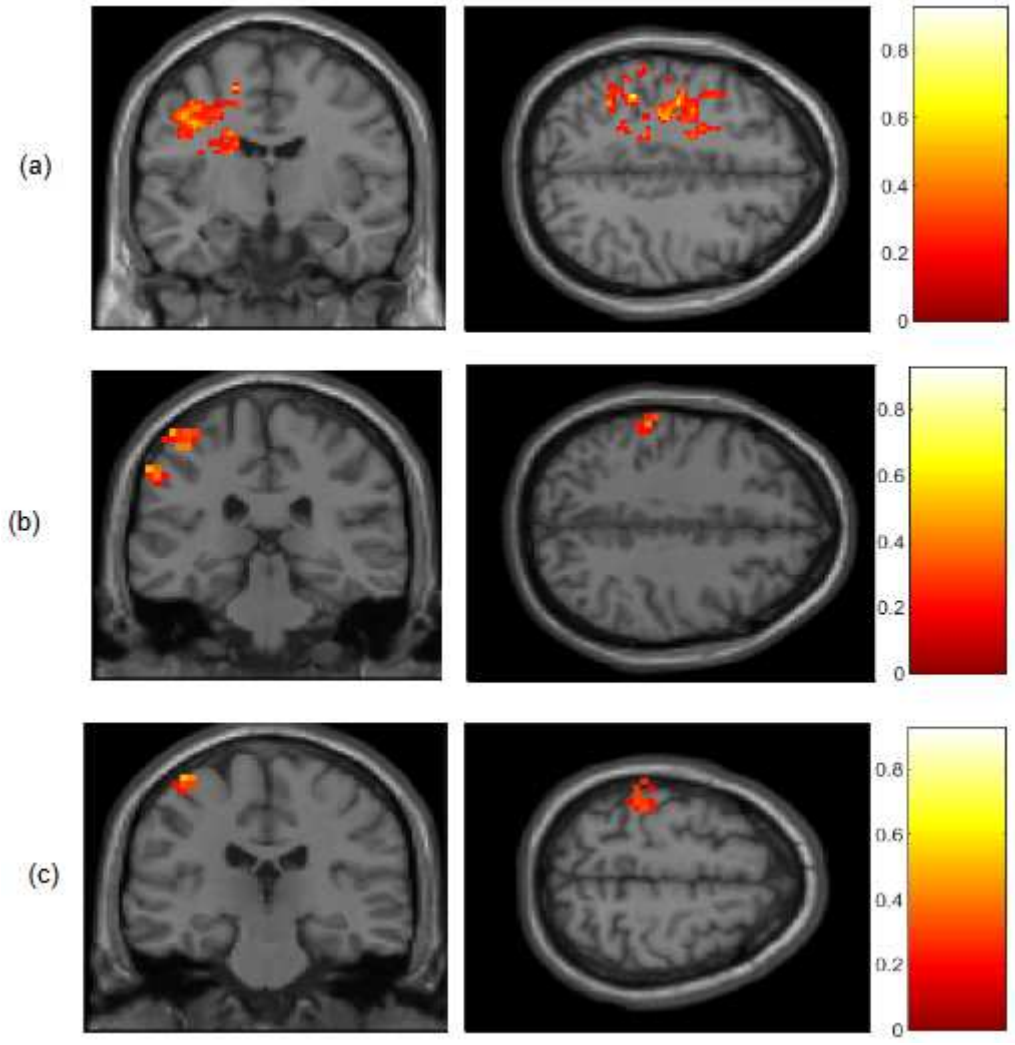

Figure A2. Statistical maps indicating t-test (FWER p<0.001) results of the z-score of the amplitude of fluctuation differences for (**a**) BOLD; (**b**) HbO and (**c**) HbR signals for the group subjects (N = 9) during the contralateral finger movements in coronal and axial views. All results were mapped onto standard space (MNI).

References

1. E. Hernandez-Martin and J. L. Gonzalez-Mora, "Diffuse optical tomography in the human brain: A briefly review from the neurophysiology to its applications," Brain Science Advances, vol. 6, no. 4, pp. 289–305, Dec. 2020, doi: 10.26599/BSA.2020.9050014.
2. E. Hernandez-Martin, F. Marcano, O. Casanova, C. Modroño, J. Plata-Bello, and J. L. González-Mora, "Comparing diffuse optical tomography and functional magnetic resonance imaging signals during a cognitive task: pilot study," vol. 4, pp. 015003-4–15, 2017, [Online]. Available: http://dx.doi.org/10.1117/1.NPh.4.1.015003
3. H.-M. Estefania, M. Cristian, J. Niels, and G.-M. J. Luis, "Does the diffuse optical tomography have more spatial sensitivity than fMRI to measure functional changes at cerebral gyri level?," in Optics and the Brain, Optical Society of America, 2020, pp. BM2C-4.
4. E. Hernandez-Martin, F. Marcano, C. Modroño, N. Janssen, and J. L. González-Mora, "Diffuse optical tomography to measure functional changes during motor tasks: a motor imagery study," Biomed Opt Express, vol. 11, no. 11, pp. 6049–6067, 2020, doi: 10.1364/BOE.399907.
5. F. B. Haeussinger, T. Dresler, S. Heinzel, M. Schecklmann, A. J. Fallgatter, and A.-C. Ehlis, "Reconstructing functional near-infrared spectroscopy (fNIRS) signals impaired by extra-cranial confounds: an easy-to-use filter method," Neuroimage, vol. 95, pp. 69–79, 2014.
6. J. Virtanen, T. E. J. Noponen, and P. Meriläinen, "Comparison of principal and independent component analysis in removing extracerebral interference from near-infrared spectroscopy signals," J Biomed Opt, vol. 14, no. 5, p. 54032, 2009.
7. R. A. Poldrack, "Region of interest analysis for fMRI.," Soc Cogn Affect Neurosci, vol. 2, no. 1, pp. 67–70, Mar. 2007, doi: 10.1093/scan/nsm006.
8. J. Ashburner et al., "SPM8 Manual Functional Imaging Laboratory," Wellcome Trust Centre for Neuroimaging, Institute of Neurology, UCL, 2008.
9. G. H. Klem, H. O. Lüders, H. H. Jasper, and C. Elger, "The ten-twenty electrode system of the International Federation," Electroencephalogr Clin Neurophysiol, vol. 52, no. 3, pp. 3–6, 1999.
10. E. Hernandez-Martin and J. L. Gonzalez-Mora, "Diffuse Optical Tomography Using Bayesian Filtering in the Human Brain," Applied Sciences, vol. 10, no. 10, p. 3399, 2020.
11. Y. Zang, T. Jiang, Y. Lu, Y. He, and L. Tian, "Regional homogeneity approach to fMRI data analysis," Neuroimage, vol. 22, no. 1, pp. 394–400, 2004.
12. M. G. Kendall, "Rank correlation methods.," 1948.
13. Y. Lv, D. S. Margulies, A. Villringer, and Y.-F. Zang, "Effects of finger tapping frequency on regional homogeneity of sensorimotor cortex," PLoS One, vol. 8, no. 5, p. e64115, 2013.
14. S. P. Koch et al., "High-resolution optical functional mapping of the human somatosensory cortex," Front Neuroenergetics, vol. 2, p. 12, 2010.
15. R. Yuan, X. Di, E. H. Kim, S. Barik, B. Rypma, and B. B. Biswal, "Regional homogeneity of resting-state fMRI contributes to both neurovascular and task activation variations," Magn Reson Imaging, vol. 31, no. 9, pp. 1492–1500, 2013.
16. T. J. Huppert, R. D. Hoge, S. G. Diamond, M. A. Franceschini, and D. A. Boas, "A temporal comparison of BOLD, ASL, and NIRS hemodynamic responses to motor stimuli in adult humans," Neuroimage, vol. 29, no. 2, pp. 368–382, Jan. 2006, doi: 10.1016/j.neuroimage.2005.08.065.
17. R. Kurth et al., "fMRI shows multiple somatotopic digit representations in human primary somatosensory cortex," Neuroreport, vol. 11, no. 7, 2000, [Online]. Available: https://journals.lww.com/neuroreport/Fulltext/2000/05150/fMRI_shows_multiple_somatotopic_digit.26.aspx
18. R. Schweizer, D. Voit, and J. Frahm, "Finger representations in human primary somatosensory cortex as revealed by high-resolution functional MRI of tactile stimulation," Neuroimage, vol. 42, no. 1, pp. 28–35, 2008, doi: https://doi.org/10.1016/j.neuroimage.2008.04.184.

    E. M. Gordon et al., "A somato-cognitive action network alternates with effector regions in motor cortex," Nature, vol. 617, no. 7960, pp. 351–359, 2023, doi: 10.1038/s41586-023-05964-2.

 doi:10.20944/preprints202309.1247.v1